

RAMAN AND IR SPECTROSCOPIC STUDIES OF ALUNITE-SUPERGROUP COMPOUNDS CONTAINING AI, Cr³⁺, Fe³⁺ AND V³⁺ AT THE B SITE

PAMELA J. MURPHY

*Centre for Earth and Environmental Science Research and School of Earth Sciences and Geography, Kingston University,
 Penrhyn Road, Kingston upon Thames, Surrey KT1 2EE, UK*

ADRIAN M.L. SMITH

*Department of Mineralogy, The Natural History Museum, Cromwell Road, London, SW7 5BD,
 Davy Faraday Research Laboratory, The Royal Institution of Great Britain, 21 Albemarle Street, London, W1S 4BS,
 and Research School of Earth Sciences at UCL–Birkbeck, University of London, Malet Street, London, WC1E 7HX, UK*

KAREN A. HUDSON-EDWARDS[§]

Research School of Earth Sciences at UCL–Birkbeck, University of London, Malet Street, London, WC1E 7HX, UK

WILLIAM E. DUBBIN

Department of Mineralogy, The Natural History Museum, Cromwell Road, London, SW7 5BD, UK

KATE WRIGHT[¶]

Davy Faraday Research Laboratory, The Royal Institution of Great Britain, 21 Albemarle Street, London, W1S 4BS, UK

ABSTRACT

Raman and IR spectroscopies, X-ray diffraction and chemical analysis have been used to characterize synthetic compounds of the alunite supergroup of formula $AB_3(\text{SO}_4)_2(\text{OH})_6$, with $A = \text{Na}^+, \text{K}^+, \text{H}_3\text{O}^+$ and $B = \text{Al}, \text{Cr}^{3+}, \text{Fe}^{3+}, \text{V}^{3+}$. For each A-site cation, the proportion of B-site vacancies decreases in the same order as the effective ionic radius of the B-site cations ($\text{Al} > \text{Cr} > \text{Fe} > \text{V}$). Raman and IR spectra of the compounds with $B = \text{Al}$ and Fe^{3+} (alunite- and jarosite-group phases) show very close agreement with previously published spectra. The spectra for Cr- and V-based analogues show similarities to the alunite- and jarosite-group phases, and particularly the latter. The Raman and IR spectra are similar in the high-wavenumber ranges (around 3400–3500 cm⁻¹), but are different in the intermediate and, particularly, the lower ranges, <700 cm⁻¹, probably owing to the different responses of Raman and IR to SO_4 and metal–O (M –O) group symmetries. The a parameter correlates well with $\nu_1\text{SO}_4$, $\nu_2\text{SO}_4$ and $\nu_4\text{SO}_4$ Raman and $\nu_3\text{SO}_4$ IR wavenumbers. There are differences in the OH-stretching regions, and shifts in the main νSO_4 and M –O peaks of the alunite-group phases, and Cr-, Fe- and V-based analogues with substitution of K, Na or H_3O at the A site in the Raman and IR spectra. Raman and IR spectroscopies are therefore useful in distinguishing these compounds.

Keywords: alunite supergroup, jarosite group, chromium, vanadium, Raman, infrared spectra, X-ray diffraction.

SOMMAIRE

Nous nous sommes servis de la spectroscopie Raman, la spectroscopie infrarouge, la diffraction X et l'analyse chimique pour caractériser les composés synthétiques du supergroupe de l'alunite, dont la formule générale est $AB_3(\text{SO}_4)_2(\text{OH})_6$, avec $A = \text{Na}^+, \text{K}^+, \text{H}_3\text{O}^+$ et $B = \text{Al}, \text{Cr}^{3+}, \text{Fe}^{3+}, \text{V}^{3+}$. Pour chaque cation au site A, la proportion de lacunes au site B diminue dans la même séquence que le rayon ionique du cation logeant au site B ($\text{Al} > \text{Cr} > \text{Fe} > \text{V}$). Les spectres de Raman et IR de ces composés ayant $B = \text{Al}$ et Fe^{3+} , c'est-à-dire les composés des groupes alunite et jarosite, concordent très étroitement avec les spectres déjà

[§] E-mail address: k.hudson-edwards@bbk.ac.uk

[¶] Present address: Nanochemistry Research Institute, Department of Applied Chemistry, Curtin University of Technology, GPO Box U1987, Perth, West Australia 6845, Australia.

publiés. Les spectres des analogues ayant Cr et V au site *B* ressemblent aux spectres des composés des groupes alunite et jarosite, et surtout à ces derniers. Les spectres Raman et IR sont semblables dans la région des spectres ayant des nombres d'onde élevés (dans la région 3400–3500 cm⁻¹), mais sont distincts dans la région intermédiaire et, en particulier, dans la région des faibles nombres d'onde, <700 cm⁻¹, probablement à cause des réponses différentes des spectres Raman et infrarouges aux symétries des groupes SO₄ et aux liaisons métal-O (*M*-O). Le paramètre *a* montre une bonne corrélation avec les nombres d'onde $\nu_1\text{SO}_4$, $\nu_2\text{SO}_4$ et $\nu_4\text{SO}_4$ du spectre Raman, et $\nu_4\text{SO}_4$ du spectre IR. Il y a des différences dans les spectres Raman et IR dans la région de l'étirement OH, et des déplacements dans les pics principaux νSO_4 et *M*-O des phases du groupe de l'alunite, et de leurs analogues à base de Cr, Fe et V avec substitution au site *A* impliquant K, Na ou H₃O. Les spectres de Raman et infrarouges sont donc utiles pour distinguer ces composés.

(Traduit par la Rédaction)

Mots-clés: supergroupe de l'alunite, groupe de la jarosite, chrome, vanadium, spectres Raman, spectres infrarouges, diffraction X.

INTRODUCTION

Minerals of the alunite supergroup occur in contaminated environments such as mine wastes, but also more widely in archeological sites, acid sulfate soils, saline lakes, hot springs and on Mars (Rewitzer & Hochleitner 1989, Hayashi 1994, Hudson-Edwards *et al.* 1999, Dutrizac & Jambor 2000, Elwood Madden *et al.* 2004, Klingelhöfer *et al.* 2004). In these environments, jarosite-group minerals scavenge potentially toxic elements such as As and Cr, and store significant amounts of H₂O (Kubisz 1970, Härtig *et al.* 1984, Ripmeester *et al.* 1986, Baron & Palmer 2002, Savage *et al.* 2005, Squyres *et al.* 2006). Jarosite-group minerals are also used in metallurgical processes to remove unwanted iron and improve metal concentrates (Dutrizac & Jambor 2000, Jiang & Lawson 2006). Members of the alunite group occur as secondary minerals after low-temperature weathering of Al-rich minerals (*e.g.*, feldspars), in hydrothermal veins and in lacustrine environments (Scott 1987, Stoffregen & Alpers 1992, Stoffregen *et al.* 2000). Characterization of these minerals in these widely ranging environments is therefore important and desirable, as their unique structure reflects the geochemical environment of formation and governs their potential for further assimilation of toxins.

Although Raman and IR spectroscopic analyses have been carried out previously on alunite and natroalunite, and jarosite and natrojarosite, no studies have to date been carried out on end-member hydroniumjarosite and hydroniumalunite, or with the analogous compounds in which the *B* site is occupied by Cr and V. Analysis of a range of *A*- and *B*-site-substituted alunite-supergroup phases will allow a better understanding of both their structures and associated vibrational spectra, and may help to distinguish these compounds. With these aims, we have prepared synthetic alunite and jarosite compounds, studied them with Raman and IR vibrational spectroscopy, and characterized them by chemical analysis and X-ray diffraction (XRD). We use synthetic compounds to achieve sample purity and to control the conditions of formation, in keeping with

previous work by others (*e.g.*, Sasaki & Konno 2000, Sasaki *et al.* 1998, Grohol & Nocera 2002, 2007). In this paper, we build on our previous work on the structure, dissolution and incorporation of potentially toxic elements in natural and synthetic members of the alunite supergroup and computational models relevant to these materials (Smith *et al.* 2006a, b, c, Hudson-Edwards *et al.* 2008).

BACKGROUND INFORMATION

Members of the isostructural alunite and jarosite groups of minerals have a general formula of $AB_3(\text{TO}_4)_2(\text{OH})_6$, where *A* represents cations with a coordination number ≥ 9 (Na⁺, K⁺, NH₄⁺, H₃O⁺), *B* represents cation sites with octahedral (O) coordination (Al in members of the alunite group, Fe³⁺ in members of the jarosite group, but also Ga, Cr³⁺ and V³⁺, forming Ga-, Cr- and V-based analogues of the alunite supergroup), and *T* represents cation sites with tetrahedral (T) coordination (in general SO₄, but also CrO₄ and AsO₄: Jambor 1999, Hawthorne *et al.* 2000). Most members of this supergroup show a non-ideal composition. Substitution of H₃O⁺ at the *A* site appears to be ubiquitous (15–20% H₃O⁺ was suggested by Brophy & Sheridan 1965), although the exact proportions appear to be highly variable, especially in low-temperature varieties. Vacancies at the *B* site also occur, as does protonated H₂O in the form of hydronium, charge balancing Fe or Al deficiencies (Kubisz 1970, Härtig *et al.* 1984, Ripmeester *et al.* 1986, Alpers *et al.* 1989). The chemical formula of alunite-supergroup phases is therefore more correctly written as $(\text{H}_3\text{O})_{1-x} \text{A}_x \text{B}_{3-y} [\text{OH}]_{6-3y} (\text{H}_2\text{O})_{3y} (\text{TO}_4)_2$. Alunite-supergroup minerals have C_{3v}⁵ symmetry owing to the bonding of SO₄ tetrahedra with one O atom bound to Al or Fe octahedra (Adler & Kerr 1965, Sasaki *et al.* 1998, Frost *et al.* 2005b). Their space group is D_{3d}⁵ (Wang *et al.* 1965, Menchetti & Sabelli 1976).

Raman and IR spectroscopies can give information on the stretching and bending vibrations associated with the interactions of atoms in minerals and other materials. Several researchers have used Raman and IR spectroscopy to study natural and synthetic alunite-

supergroup minerals and compounds (*e.g.*, Omori & Kerr 1963, Adler & Kerr 1965, Powers *et al.* 1975, Serna *et al.* 1986, Breitinger *et al.* 1997, 1998, Sasaki *et al.* 1998, Drouet & Navrotsky 2003, Drouet *et al.* 2004, Bishop & Murad 2005, Frost *et al.* 2005a, 2005b, 2005c, 2006a, 2006b, Savage *et al.* 2005, Hudson-Edwards *et al.* 2008). The rationale for these studies is that substitution in the structure of alunite and jarosite will affect the vibrational IR and Raman spectra, and the changes observed will depend both on the substituting ions and on their position within the structure, as well as on temperatures of formation. Each alunite-group and jarosite-group compound should, therefore, have distinct Raman and IR spectra, which can be used to fingerprint the mineral or compound and give important information on its structure and site symmetry.

Several authors have carried out Raman and IR spectroscopic studies on natural and synthetic members of the alunite and jarosite groups. Powers *et al.* (1975) published IR spectra of synthetic jarosite. Serna *et al.* (1986) reported infrared spectra and Raman data for alunite, natroalunite and hydroniumalunite, and for jarosite, natrojarosite, hydroniumjarosite and ammonio-jarosite. Sasaki *et al.* (1998) published Raman and FTIR spectra for synthetic K, Na, NH₄, Ag and Pb members of the jarosite group, but they did not cover the OH-stretching range with the Raman spectra. There are considerable differences between the data of Serna *et al.* (1986) and those of Sasaki *et al.* (1998), an observation that is largely ignored by the latter authors. Drouet & Navrotsky (2003) and Grohol *et al.* (2003) used FTIR to study members of the jarosite – natrojarosite – hydroniumjarosite solid-solution series, and Drouet *et al.* (2004) applied FTIR spectroscopy, among other techniques, to the study of synthetic jarosite–alunite and

natrojarosite–natroalunite solid-solution. Breitinger *et al.* (1997) published Raman and IR spectra for alunite, along with a group analysis of the symmetry, and Breitinger *et al.* (1998) obtained Raman spectra of synthetic jarosite, hydroniumjarosite, and their deuterated versions. Grohol & Nocera (2002) carried out IR characterization of synthetic hydrothermal Na–K–V-bearing analogues of alunite, and Grohol & Nocera (2007) did that for synthetic jarosite–hydroniumjarosite.

METHODS AND MATERIALS

Synthesis of alunite-group and jarosite-group compounds

Alunite-supergroup compounds with A sites filled with K, Na and H₃O and B sites filled with Al, Cr, Fe and V were synthesized using the volumes, reagents, temperatures and stirring times indicated in Table 1. For all compounds, the prepared solutions were placed in covered beakers and heated in an autoclave with constant stirring (400 rpm) at 1 atm. The precipitate thus formed was allowed to cool and settle, and the supernatant solution was decanted. The precipitate was then washed several times with ultrapure water (18 MΩ cm⁻¹), then dried at 110°C for 24 h. All reagents were AnalR grade (Aldrich).

Chemical analysis

For quantitative total elemental analysis of the Al-, Fe- and V-bearing alunite-supergroup compounds, approximately 30 mg of the dried synthetic compound was dissolved in a polypropylene beaker by adding HCl dropwise until no solid remained. For the Cr-bearing

TABLE 1. CONDITIONS OF SYNTHESIS OF ALUNITE-SUPERGROUP COMPOUNDS

Compound	Volume of solution	Reagents	Temperature of synthesis	Duration*	Reference
K-Al	50 mL	0.3 M K ₂ SO ₄ + 0.1 M Al ₂ (SO ₄) ₃ •18H ₂ O	145°C	24 h (a)	(1)
Na-Al	50 mL	0.3 M Na ₂ SO ₄ + 0.1 M Al ₂ (SO ₄) ₃ •18H ₂ O	145°C	24 h (a)	(1)
H ₃ O-Al	50 mL	1.0 M Al ₂ (SO ₄) ₃ •18H ₂ O	145°C	24 h (a)	(1)
K-Cr	10 mL	0.25 M K ₂ SO ₄ + 0.1 M Cr ₂ (SO ₄) ₃	230°C	16 h (s)	adapted from (4)
Na-Cr	10 mL	0.25 M Na ₂ SO ₄ + 0.1 M Cr ₂ (SO ₄) ₃	230°C	16 h (s)	adapted from (4)
H ₃ O-Cr	10 mL	0.67 M Cr ₂ (SO ₄) ₃	25°C	16 h (s)	based on (4)
K-Fe	100 mL	1.0 M KOH + 0.351 M Fe ₂ (SO ₄) ₃ •5H ₂ O	95°C	4 h (s)	(2), (5)
Na-Fe	50 mL	0.3 M Na ₂ SO ₄ , 0.1 M Fe ₂ (SO ₄) ₃ + 0.01 M H ₂ SO ₄	135°C	24 h (a)	adapted from (2), (5)
H ₃ O-Fe	60 mL	0.27 M Fe ₂ (SO ₄) ₃	135°C	24 h (a)	adapted from (2), (5)
K-V	10 mL	Reagent-grade VCl ₃ was dissolved in distilled water to give a 0.4 M V ³⁺ solution; 0.4 VCl ₃ + 0.4 M K ₂ SO ₄	145°C	24 h (a)	(3)
Na-V	10 mL	Reagent-grade VCl ₃ was dissolved in distilled water to give a 0.4 M V ³⁺ solution; 0.4 VCl ₃ + 0.4 M Na ₂ SO ₄	145°C	24 h (a)	(3)
H ₃ O-V	10 mL	0.4 M Li ₂ SO ₄ + 0.4 M VCl ₃	145°C	24 h (a)	(3)

Alunite-supergroup compounds are labeled according to the occupant of the A and the B sites. References to the literature: (1) Ripmeester *et al.* (1986), (2) Baron & Palmer (1996), (3) Dutrizac & Chen (2003), (4) Dutrizac & Chen (2005), (5) Smith *et al.* (2006c). * Duration of stirring (s) or of autoclave experiment (a).

compounds, approximately 30 mg was dissolved in 4 mL HCl and 1 mL HNO₃ using a MARS microwave digestion instrument. The temperature was increased to 200°C in 25 min and held at this temperature for a further 25 min, using a power setting of 300 W and pressure of 350 to 360 psi. After digestion, the solutions were then made up to 50 mL with 2% HNO₃ and, depending on the type of compound, analyzed for Al, Cr, K, Na, Fe, S and V by inductively coupled plasma – optical emission spectrometry (ICP–OES) on a Varian Vista-Pro (axial configuration) using a simultaneous solid-state detector (CCD).

X-ray diffraction

The jarosite-group products of precipitation were identified using powder XRD analysis at 25°C with a Philips PW1050 vertical powder diffractometer utilizing Co K α_1 and K α_2 ($\lambda = 1.7903 \text{ \AA}$) radiation at 35 kV and 30 mA. The alunite-group and Cr- and V-based products of precipitation were identified using powder XRD analysis in Bragg–Brentano reflection geometry on a Bruker D8 diffractometer equipped with a position-sensitive detector and operating at 40 kV and 40 mA at 25°C. The diffractometer was fitted with a Ge (111) monochromator, producing CuK α_1 radiation ($\lambda = 1.54056 \text{ \AA}$). The monochromator slit was 2 mm, the exit slit was 0.6 mm. The sample was mounted on a Bruker zero-background silicon (510) sample holder. For all XRD scans, the starting and the final 2 θ angles were 5 and 110°, respectively. The step size was 0.007° 2 θ , with 3.5 seconds spent per step.

Unit-cell parameters were calculated with a Rietveld refinement using GSAS (Larson & Von Dreele 1998) and the “model free” Le Bail method (Le Bail *et al.* 1988), where individual “|F_{obs}|” are obtained by Rietveld decomposition from arbitrarily identical values. In addition to the structure factors, free refinement was made of the unit-cell parameters, constrained according to the rhombohedral symmetry of the space group in the centered hexagonal setting, background, profile parameters, and the instrumental zero-point. In all cases, a pseudo-Voigt profile was used.

Raman and infrared spectroscopy

Laser Raman microspectroscopic analyses were carried out using a Renishaw RM1000 Raman spectrometer equipped with a thermoelectrically cooled CCD detector and a 514.5 nm Ar ion laser. The instrument was calibrated daily on a silicon standard at 520.5 cm⁻¹. The system was operated in confocal mode with the laser focused on the sample through the objective lens ($\times 50 - \times 100$) of an Olympus petrological microscope. Under these conditions, the Raman analysis was restricted to an area less than 2 μm in diameter. The laser power was reduced using neutral-density filters and was typically between 1 mW and *ca.* 220 μW at

the sample. Samples were inspected optically for any laser damage, and none was observed. Spectra were recorded over the wavenumber range 100 to 4000 cm⁻¹ using an integration time of 10–45 s (total analysis time in the range 100–450 s). Errors on channel wavelength positions were less than 0.1 cm⁻¹.

Peak fitting was performed using Galactic GRAMS/32 software, which uses a mixed Gaussian–Lorentzian curve. In order to test the variability of the spectra, at least 10 spectra were obtained in the low-wavenumber region for each sample. The variation between individual spectra was small: for the Na–K-bearing jarosite-group compounds, for example, 10 spectra gave an average wavenumber for the 1010 cm⁻¹ band of 1010.58 cm⁻¹ (1σ 0.377 cm⁻¹), and a mean band-width (FWHM) of 8.56 cm⁻¹ (1σ 0.424 cm⁻¹). The samples were therefore assumed to be homogeneous.

Infrared spectroscopy (IR) spectra were collected with a PerkinElmer Spectrum One FTIR spectrometer using the KBr pellet (13 mm) technique (McMillan & Hofmeister 1988). Spectra were recorded in transmission mode immediately after pellet preparation; the scanning range was 400–4000 cm⁻¹, with a resolution of 4 cm⁻¹, and five scans were accumulated for each sample.

RESULTS AND DISCUSSION

Composition and cell dimensions of synthetic alunite- and jarosite-group compounds

The precipitates were identified as end-member K-, Na- and H₃O-bearing alunite- and jarosite-group compounds by comparing their powder-diffraction patterns with those reported in International Centre for Diffraction Data Powder Diffraction Files (ICDD PDF) (Fig. 1, Table 2). Where no ICDD PDF files were available, previously published XRD data were used to identify the compounds (*e.g.*, Dutrizac & Chen 2003, 2005) (Table 2). All peaks produced by the precipitates relate to the structure of the respective alunite- and jarosite-group phases; the absence of additional peaks indicates that no other phases are present at detectable levels. The calculated unit-cell parameters of the alunite- and jarosite-group compounds and of Cr- and V-bearing analogues are presented in Table 2.

Mole percentages of the A-, B- and T-site elements in the alunite-supergroup compounds were determined using the bulk-composition data and the modified formula of Kubisz (1970). Deficiencies at the B site are expressed by the B:SO₄ molar ratio, which typically is significantly lower than the ideal of 3:2 (Kubisz 1970), with values as low as 2.20:2 to 2.57:2 (Härtig *et al.* 1984). These deficiencies are charge-balanced by the incorporation of H₂O (hydronium) into the structure and protonation of OH⁻ groups (Kubisz 1970, Härtig *et al.* 1984, Ripmeester *et al.* 1986) (Table 2). The formulas in Table 2 suggest that our alunite-supergroup

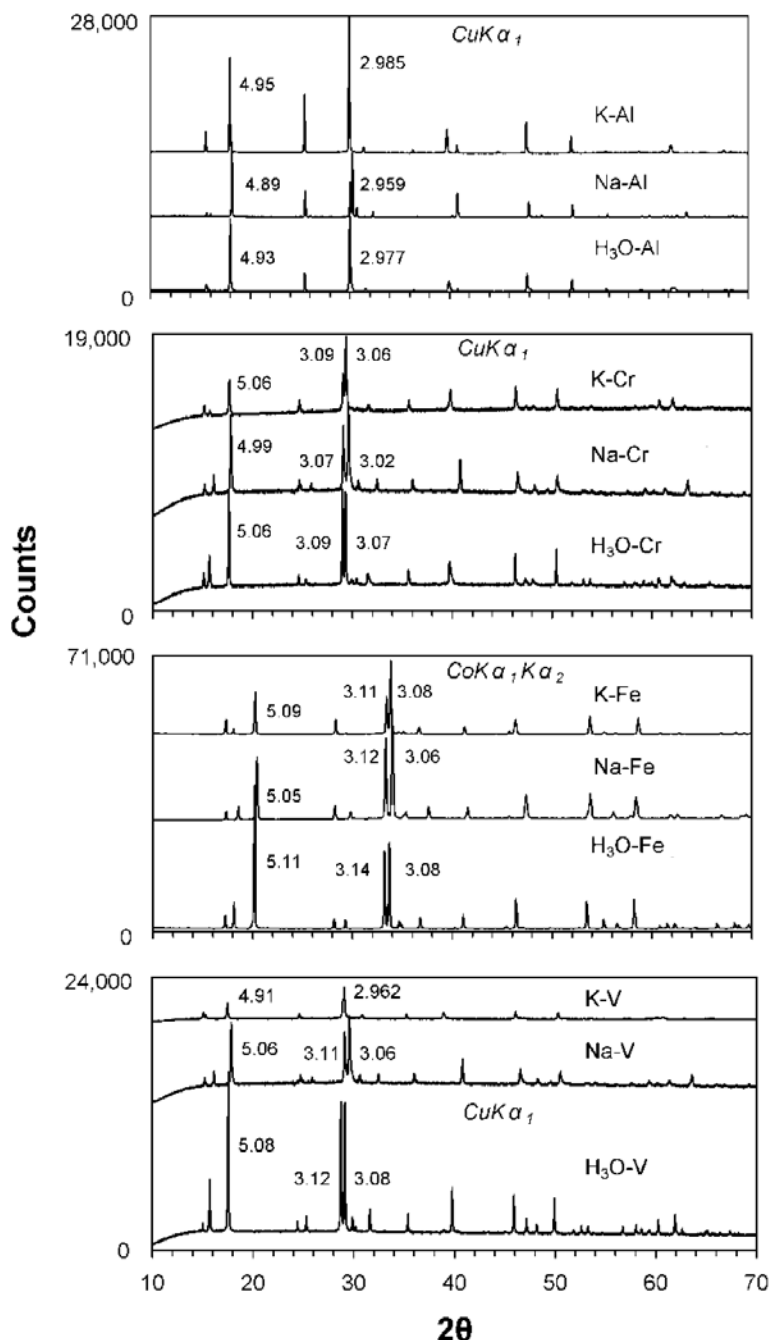


FIG. 1. XRD patterns of synthetic alunite-supergroup compounds. The dominant *d*-values are indicated for each compound, which are labeled according to the occupant of the *A* and the *B* sites.

TABLE 2. ELEMENTAL CONCENTRATIONS, UNIT-CELL PARAMETERS (WHERE AVAILABLE) AND ICDD PDF FILE OR REFERENCES FOR SYNTHETIC ALUNITE AND JAROSITE-GROUP COMPOUNDS AND Cr- and V-BASED ANALOGUES

Compound	Nominal formula	Actual formula	<i>a</i> (Å)	<i>c</i> (Å)	ICDD PDF or reference
K-Al	KAl ₃ (SO ₄) ₂ (OH) ₆	K _{0.78} (H ₃ O) _{0.22} Al _{2.17} (SO ₄) ₂ (OH) _{3.51} (H ₂ O) _{2.49}	7.0074	17.1190	86-2165
Na-Al	NaAl ₃ (SO ₄) ₂ (OH) ₆	Na _{0.82} (H ₃ O) _{0.18} Al _{2.33} (SO ₄) ₂ (OH) _{3.99} (H ₂ O) _{2.01}	6.9916	16.6517	41-1467
H ₃ O-Al	(H ₃ O)Al ₃ (SO ₄) ₂ (OH) ₆	(H ₃ O)Al _{2.76} (SO ₄) ₂ (OH) _{5.28} (H ₂ O) _{0.72}	6.9911	17.0062	70-3158
K-Cr	KCr ₃ (SO ₄) ₂ (OH) ₆	K _{0.68} (H ₃ O) _{0.32} Cr _{2.26} (SO ₄) ₂ (OH) _{3.78} (H ₂ O) _{2.22}	7.2543(7)	17.0712(17)	18-0381, (2)
Na-Cr	NaCr ₃ (SO ₄) ₂ (OH) ₆	Na _{0.86} (H ₃ O) _{0.14} Cr _{2.50} (SO ₄) ₂ (OH) _{4.50} (H ₂ O) _{1.50}	7.2268(9)	16.5633(20)	18-0381, (2)
H ₃ O-Cr	(H ₃ O)Cr ₃ (SO ₄) ₂ (OH) ₆	(H ₃ O)Cr _{2.82} (SO ₄) ₂ (OH) _{5.46} (H ₂ O) _{0.54}	7.2497(7)	17.0500(15)	18-0381, (2)
K-Fe	KFe ₃ (SO ₄) ₂ (OH) ₆	K _{0.84} (H ₃ O) _{0.16} Fe _{2.48} (SO ₄) ₂ (OH) _{4.38} (H ₂ O) _{1.62}	7.3137(6)	17.0730(5)	22-0827
Na-Fe	NaFe ₃ (SO ₄) ₂ (OH) ₆	Na _{0.76} (H ₃ O) _{0.24} Fe _{2.68} (SO ₄) ₂ (OH) _{5.04} (H ₂ O) _{0.96}	not calculated		30-1203
H ₃ O-Fe	(H ₃ O)Fe ₃ (SO ₄) ₂ (OH) ₆	(H ₃ O)Fe _{2.93} (SO ₄) ₂ (OH) _{5.79} (H ₂ O) _{0.21}	7.3577(1)	17.0149(4)	21-0932
K-V	KV ₃ (SO ₄) ₂ (OH) ₆	K _{0.74} (H ₃ O) _{0.26} V _{2.74} (SO ₄) ₂ (OH) _{5.22} (H ₂ O) _{0.78}	7.2614(51)	17.0068(54)	(1)
Na-V	NaV ₃ (SO ₄) ₂ (OH) ₆	Na _{0.62} (H ₃ O) _{0.38} V _{2.77} (SO ₄) ₂ (OH) _{5.31} (H ₂ O) _{0.69}	7.3003(8)	16.8889(18)	(1)
H ₃ O-V	(H ₃ O)V ₃ (SO ₄) ₂ (OH) ₆	(H ₃ O)V _{2.96} (SO ₄) ₂ (OH) _{5.88} (H ₂ O) _{0.12}	7.3196(3)	17.0278(7)	(1)

Alunite-supergroup compounds are labeled according to the occupant of the A and the B sites. References to the literature: (1) Dutrizac & Chen (2003), (2) Dutrizac & Chen (2005). Chemical formulas were determined by HCl digestion (Al, Fe and V compounds) or HCl-HNO₃ digestion (Cr compounds), followed by ICP analysis. We applied the modified formula of Kubisz (1970).

compounds are not true end-member species, despite the observation that their structures, as revealed by XRD, match those of their respective end-member minerals. Bulk-composition data showing similar deviations from exact stoichiometry were given by Drouet *et al.* (2004), but their range of H₂O content was somewhat narrower (0.54–1.8 moles/unit formula, compared to 0.04–2.49 in this study), and their temperatures of synthesis were lower than those reported here.

For each A-site cation (Na⁺, K⁺, H₃O⁺), the proportion of B-site vacancies decrease in the order Al > Cr > Fe > V (Table 2), which broadly mirrors the size of the effective ionic radii of the B-site cations (Fe 0.645 Å and V 0.64 Å > Cr 0.615 Å > Al 0.535 Å: Shannon 1976), suggesting that the number of vacancies is inversely related to the size of the B-site cation. A similar effect was found by Drouet *et al.* (2004), who reported that the proportion of B-site vacancies decreases with increasing Fe-for-Al substitution in jarosite–alunite solid solutions. Many authors have suggested that lower temperatures of synthesis favor a higher proportion of vacancies (Alpers *et al.* 1989, Stoffregen & Alpers 1992, Swayze *et al.* 2006). The relationship between synthesis temperature (Table 1) and B-site vacancies for the alunite-supergroup compounds prepared for this study (Table 2) does not appear to confirm this hypothesis in that many of the higher-temperature compounds have a high proportion of vacancies (Fig. 2).

The alunite-supergroup compounds all have cell dimensions near 7 Å for *a* and 17 Å for *c*, in agreement with other studies (*e.g.*, Hendricks 1937, Brophy &

Sheridan 1965, Dutrizac & Jambor 1984, Kato & Miúra 1977, Dutrizac & Kaiman 1976, Stoffregen & Alpers 1992), although these dimensions are quite variable (Table 2). Variations in *a* and *c* in synthetic compounds belonging to the alunite supergroup have been attributed to several factors, including variations in hydronium content (*a* decreases and *c* increases with decreasing H₃O⁺), which can be related to the temperature of synthesis for alunite- and jarosite-group compounds with the same B-site cation (Alpers *et al.* 1989, Stoffregen & Alpers 1992), and different cations (other than hydronium) at the A and B sites (Brophy & Sheridan 1965, Alpers *et al.* 1989, Stoffregen *et al.* 2000, Drouet *et al.* 2004). Substitution at the A site will result in a much greater variation in *c* than in *a* (*e.g.*, Brophy & Sheridan 1965). Substitution at the B site has a significant effect on the *a* parameter (which increases with Fe content, for example, in the Fe–Al solid-solution series), but little or no effect on *c* (Stoffregen *et al.* 2000, Drouet *et al.* 2004). In our samples, there is no clear relationship between the A-site hydronium content of any of the different alunite- and jarosite-group compounds and their respective *a* and *c* parameters. The *a* parameter, however, exhibits a nearly linear correlation with the ionic radii of the B-site cation (Fig. 3c), but not the A-site cation (Fig. 3a), whereas the *c* parameter shows an approximately linear correlation with the ionic radius of the A-site cation (Fig. 3b) but not the B-site cation (Fig. 3d), in agreement with other studies (Menchetti & Sabelli 1976, Stoffregen *et al.* 2000, Rudolph *et al.* 2003, Bishop & Murad 2005).



FIG. 2. Relationship between temperature of synthesis and percentage of *B*-site vacancies for alunite-supergroup compounds. Symbols: ♦ alunite-group compounds, □ compounds having Cr at the *B* site, ▲ jarosite-group compounds, × compounds having V at the *B* site.

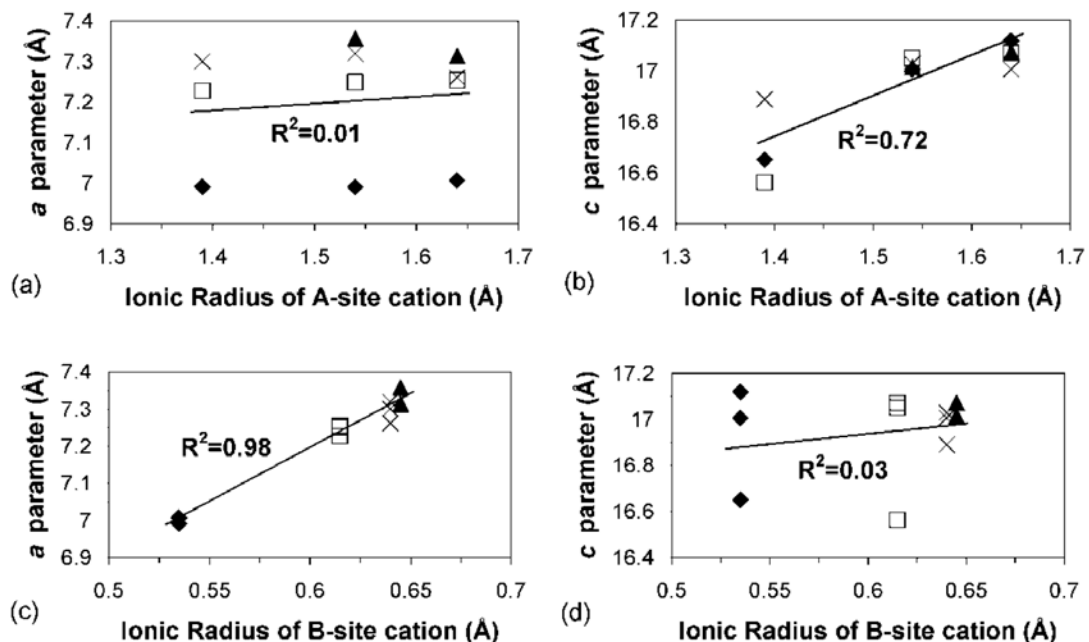


FIG. 3. X-Y plots comparing unit-cell parameter in alunite- and jarosite-group compounds and Cr and V analogues with ionic radii of A- and B-site cations. (a) The a unit-cell parameter with ionic radius of A-site cations, (b) the c unit-cell parameter with ionic radius of A-site cations, (c) the a unit-cell parameter with ionic radius of B-site cations, and (d) the c unit-cell parameter with ionic radius of A-site cations. Values of ionic radii for Al (0.535 \AA), Cr (0.615 \AA), Fe (0.645 \AA), K (1.64 \AA), Na (1.39 \AA) and V (0.64 \AA) are taken from Shannon (1976), and for H_3O (1.54 \AA) from Okada *et al.* (1987). The R^2 values of the linear fits are shown for all plots. Symbols: ♦ alunite-group compounds, □ compounds having Cr at the *B* site, ▲ jarosite-group compounds, × compounds having V at the *B* site.

The Raman spectra

Raman spectra for the alunite-supergroup compounds are shown in Figure 4 in separate plots for each *B* site, with the spectra for the *A*-site substitution shown. In Figure 4, the spectra are shown across the whole range of wavenumber, and also in more detail across each range of interest. The wavenumbers of the peaks in these spectra are listed in Table 3. These were assigned on the basis of data from Serna *et al.* (1986) and Frost *et al.* (2005a, 2006a, 2006b), and confirmed with the assignments of Sasaki *et al.* (1998). The Raman spectra show four main groups of bands: those due to OH stretching or bending vibrations ($3300 - ca. 3700 \text{ cm}^{-1}$), internal modes of the SO_4^{2-} group occurring over two regions ($430-650$ and $980-1200 \text{ cm}^{-1}$), and *B*-site M–O stretches (mostly less than 440 cm^{-1}). These are discussed in more detail below.

The OH-stretching regions separate into two bands in Al-dominant structures (Fig. 4a). Fitting of the spectra yields two Raman peaks for all of the compounds (Table 3) except the K–Cr and Na–V alunite-supergroup compounds, which are too weak to clearly resolve the peaks separately, or they may be too broad and overlap (Figs. 4b, d). The wavenumbers of the νOH band for the Al-based compounds are the highest, followed by the Cr-, Fe- and V-dominant alunite-supergroup

compounds. This is the same order observed above for the number of *B*-site vacancies, which was linked to the inverse of the magnitude of the effective radius of the *B*-site cations or temperature of synthesis.

The other OH bands do not occur in all of the synthetic compounds. The δOH (HOH bend) is present only in the Al- and Cr-dominant compounds (Table 3). Peaks assigned to γOH only occur at 992.5 cm^{-1} (alunite), 997.0 cm^{-1} (natroalunite), 998.5 cm^{-1} (K–Cr alunite-supergroup compound), 768.9 cm^{-1} (synthetic hydroniumjarosite) and 892.7 cm^{-1} (synthetic K–V alunite-supergroup compound), but not in the other compounds.

The internal modes of the free SO_4^{2-} ion give four fundamental vibrations, which occur at intermediate and low wavenumbers (in the free ion, these are: $\nu_1 983$, $\nu_2 450$, $\nu_3 1105$ and $\nu_4 611 \text{ cm}^{-1}$; Ross 1974). However, within the alunite–jarosite structure, the T_d symmetry of the tetrahedron will be reduced, removing the degeneracy of some of the vibrations, and splitting the bands (e.g., Frost *et al.* 2005a, 2005b). The D_{3d}^5 space group and C_{3v}^5 symmetry of these minerals suggests that one ν_1 , one ν_2 , two ν_3 and two ν_4 vibrations should be expected (Adler & Kerr 1965, Wang *et al.* 1965, Hug 1997, Bishop & Murad 2005, Frost *et al.* 2006b). We have assigned these numbers of vibrations for our Raman bands (Table 3), but there are some

TABLE 3. RAMAN WAVENUMBERS (cm^{-1}) OF ALUNITE-SUPERGROUP COMPOUNDS WITH THE A SITE FILLED WITH K, Na AND H_3O , AND THE B SITE FILLED WITH Al, Cr, Fe AND V

Assignment	K-Al	Na-Al	H_3O -Al	K-Cr	Na-Cr	H_3O -Cr	K-Fe	Na-Fe	H_3O -Fe	K-V	Na-V
ν_{OH}	3514.1 ¹	3487.6 ¹	3499.0 ¹	3454.9	3446.6	3464.1	3415.0	3395.0¹	3431.0	3479.9	
ν_{OH}	3476.1¹	3446.7 ¹	3466.4¹		3439.0	3391.9	3342.0	3277.0 ¹	3365.0	3406.8	3442.0
Unassigned									2522.1		
Unassigned									2420.3		
Unassigned						1602.0				1706.0	
$\nu_3(\text{SO}_4^{2-})$	1197.4 ¹		1189.6 ¹			1184.8	1157.6 ¹	1158.6 ¹	1167.7 ¹		
δOH	1155.1 ¹	1170.6 ¹	1162.4 ¹	1184.8	1181.9	1124.2					
$\nu_3(\text{SO}_4^{2-})$	1081.9¹	1090.4 ¹	1082.0¹	1119.5	1125.0	1054.2	1101.5¹	1110.8¹	1100.6¹	1111.5	1117.4
Unassigned	1052.9						1020.0	1021.0	1018.8		
Unassigned						1024.3					
$\nu_1(\text{SO}_4^{2-})$	1026.7¹	1029.0 ¹	1030.6¹	1018.4	1016.3	1022.7	1005.9¹	1010.8¹	1011.8¹	1014.7	1017.7
Unassigned	1014.0	1016.6								995.1	
γOH	992.5	997.0			998.5					768.9	892.7
$\nu_4(\text{SO}_4^{2-})$									652.4	632.6	646.9
$\nu_4(\text{SO}_4^{2-})$	656.1¹	654.7 ¹	652.9¹	638.4	637.8	635.0	623.3¹	622.7¹	619.1¹	630.9	628.8
$M-\text{O}^+$ or YOH^5	563.4 ^{1,4}	578.9 ^{1,4}									
νOH	505.5	516.4	511.2	620.6	614.9	616.6	569.6 ¹	565.4 ¹	564.5 ¹	597.7	590.2
$\nu_2(\text{SO}_4^{2-})$	488.4⁴	485.9 ⁴	486.6 ⁴	473.5	474.7	477.8	452.6 ^{2,3}	451.3 ^{2,3}	458.0 ^{2,3}	463.4	
$\nu_2(\text{SO}_4^{2-})$	387.2 ⁴	401.7 ⁴	389.9 ⁴	441.7	452.8	437.7	431.0^{2,3}	438.6^{2,3}	419.5^{2,3}	437.8	448.2
$M-\text{O}$									412.0 ¹		
$M-\text{O}$					383.4	387.9	375.3	354.3	364.1 ¹	358.5	365.2
$M-\text{O}$					297.2			299.1	294.7 ¹	281.3	305.6
$M-\text{O}^1$ or $\text{OH}-\text{O}^5$	251.6^{1,4}		248.1 ^{1,4}	261.9	292.3	266.8	222.2	225.6¹	227.1		

Peak assignments for the alunite- and jarosite-group compounds are based on Serna *et al.* (1986)¹ and Frost *et al.* (2005a³, 2006a⁴, 2006b⁵); assignments for the other alunite-supergroup compounds are inferred. The $\text{H}_3\text{O}-\text{V}$ compound did not give an interpretable spectrum. The strongest peaks for each assignment are shown in bold.

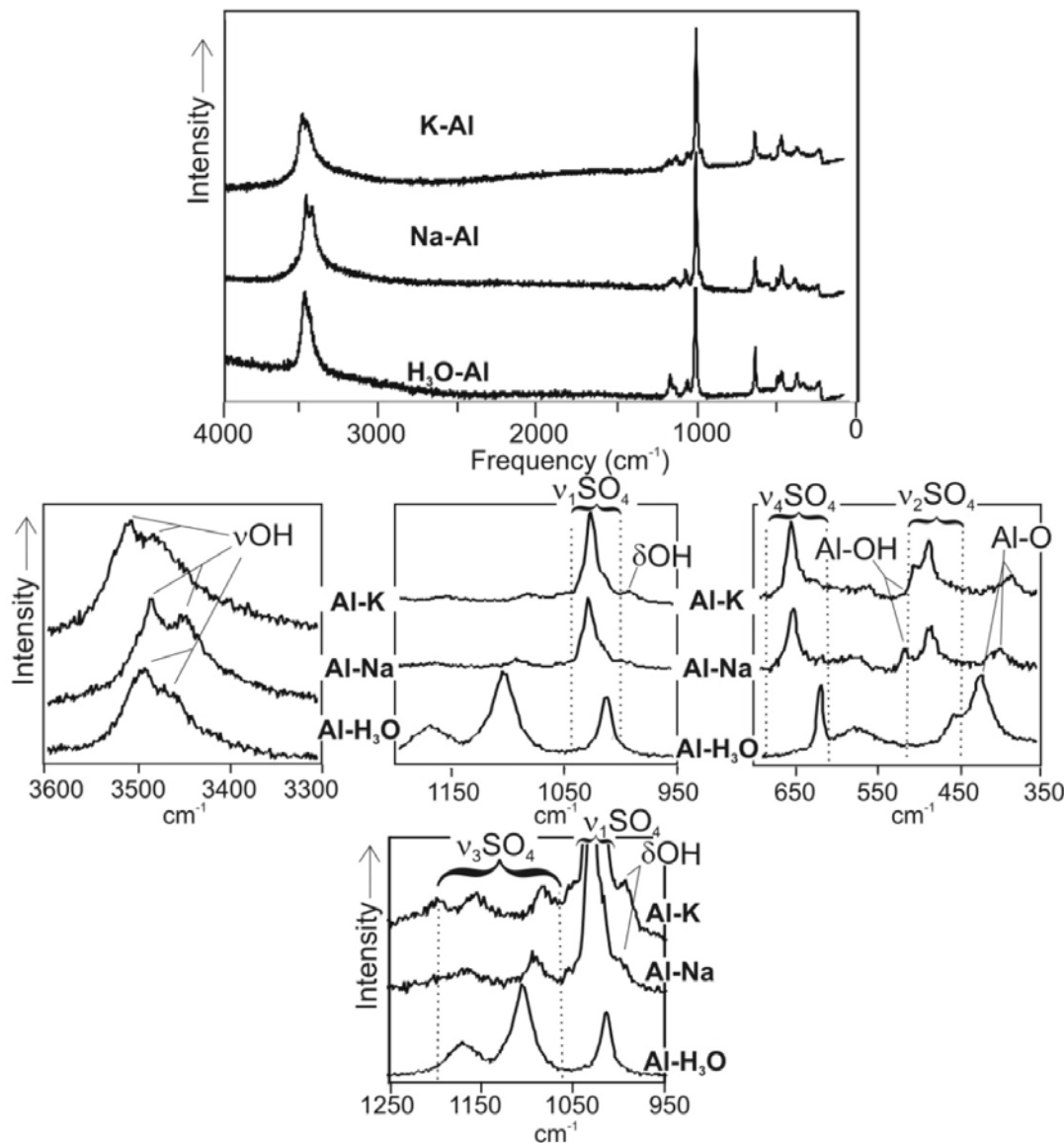


FIG. 4a. Raman spectra of synthetic alunite-group compounds. Intensity values are not shown on the y axis because the spectra have been normalized to enhance the peak contrast.

unassigned bands that may represent the band splitting described by Frost *et al.* (2005a, 2005b) (*e.g.*, 1014.0 cm^{-1} for synthetic alunite, which may be a split part of the $v_1\text{SO}_4$, Table 3).

The M–O bands represent MO_6 octahedra (described more accurately as $MO_2(\text{OH})_4$ octahedra, Breitinger *et al.* 1997). These bands occur at low wavenumbers ($<700 \text{ cm}^{-1}$) but, owing to the occurrence of v_2 and

$v_4\text{SO}_4$ bands and lattice vibrations in this region, their unequivocal assignment can be difficult. Nevertheless, two groups of peak assignments have been made for M–O vibrations for the Al- and Fe-based compounds: those between 222.2 and 305.6 cm^{-1} , and those between 354.3 and 412.0 cm^{-1} (Table 3). Frost *et al.* (2006b) assigned peaks at around 240 cm^{-1} to OH–O hydrogen bonds for alunite and natroalunite. Peaks

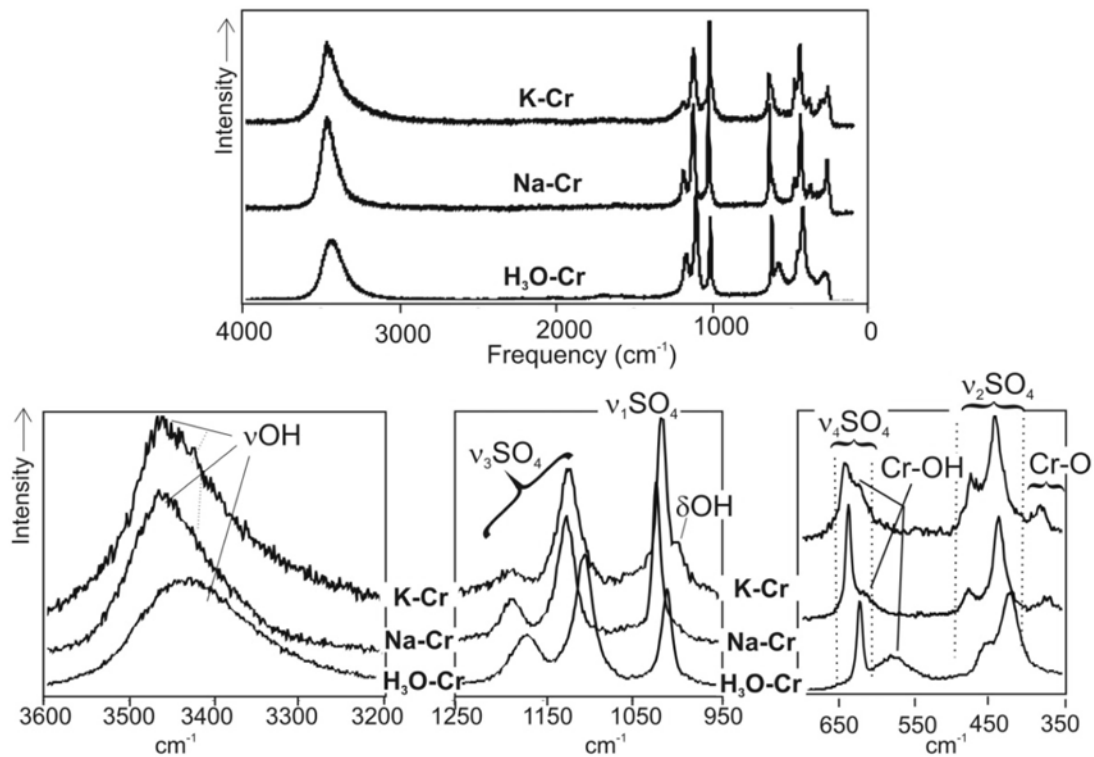


FIG. 4b. Raman spectra of synthetic Cr-based alunite-supergroup compounds. See Figure 4a for explanation.

of the Cr-dominant alunite-supergroup compound have the highest wavenumbers, followed by the K-V alunite-supergroup compound, the jarosite-group compounds and, finally, the alunite-group compounds. All the compounds also exhibit a single γ OH vibration between 505.5 and 620.6 cm^{-1} (Table 3). The γ OH peaks assigned to the Cr-dominant alunite-supergroup phases have the highest wavenumbers, and those to the alunite-group compounds, the lowest, and each B-site group have similar wavenumbers. The two peaks at 563.4 cm^{-1} and 578.9 cm^{-1} for alunite and natroalunite, respectively, are assigned either to M-O (Serna *et al.* 1986) or γ OH (Frost *et al.* 2006b).

IR SPECTRA AND COMPARISON WITH RAMAN

The IR spectra for the alunite-supergroup compounds are shown in Figure 5, and their wavenumbers are listed in Table 4. Peaks were assigned on the basis of data from Serna *et al.* (1986), Sasaki *et al.* (1998), Bishop & Murad (2005) and Frost *et al.* (2005a, 2006a, 2006b). Like the Raman spectra, the IR spectra show four main groups of bands: the OH stretching or bending vibrations, two groups of SO_4 vibrations, and M-O stretches. The measured IR range (4000–400 cm^{-1}), however,

does not extend as low as the measured Raman range (4000–200 cm^{-1}). Minerals of the alunite and jarosite groups may have bands occurring in both Raman and IR spectra, as seen in the synthetic compounds prepared for this study (Tables 3, 4). Background subtraction is usually not necessary for the Raman spectra but is complex for IR. The bands are generally narrower and easier to resolve in the Raman spectrum, with less overlap of bands.

In both the Raman and IR spectra, the OH-stretching region shows one or two bands in the compounds of alunite and jarosite groups (Table 3, 4). Peak fitting for the Raman data shows that this band is made up of at least two broad peaks. Fitting of the IR spectra, however, generally yielded only one peak (two for the natrojarosite and the K-V alunite-supergroup phase), in contrast to the two fit by other authors (*e.g.*, Serna *et al.* 1986, Bishop & Murad 2005). We do not have an explanation for this discrepancy, but suggest that it may be due to broad, overlapping bands, as in some of the Raman spectra (see above). Certain bands, such as the δ OH-bending region around 1630 cm^{-1} , are far stronger in the IR spectra than in the Raman spectra. Weak bands also occur around 2900 cm^{-1} in the IR spectra, but are not seen in the Raman spectra; these may be due to C-H

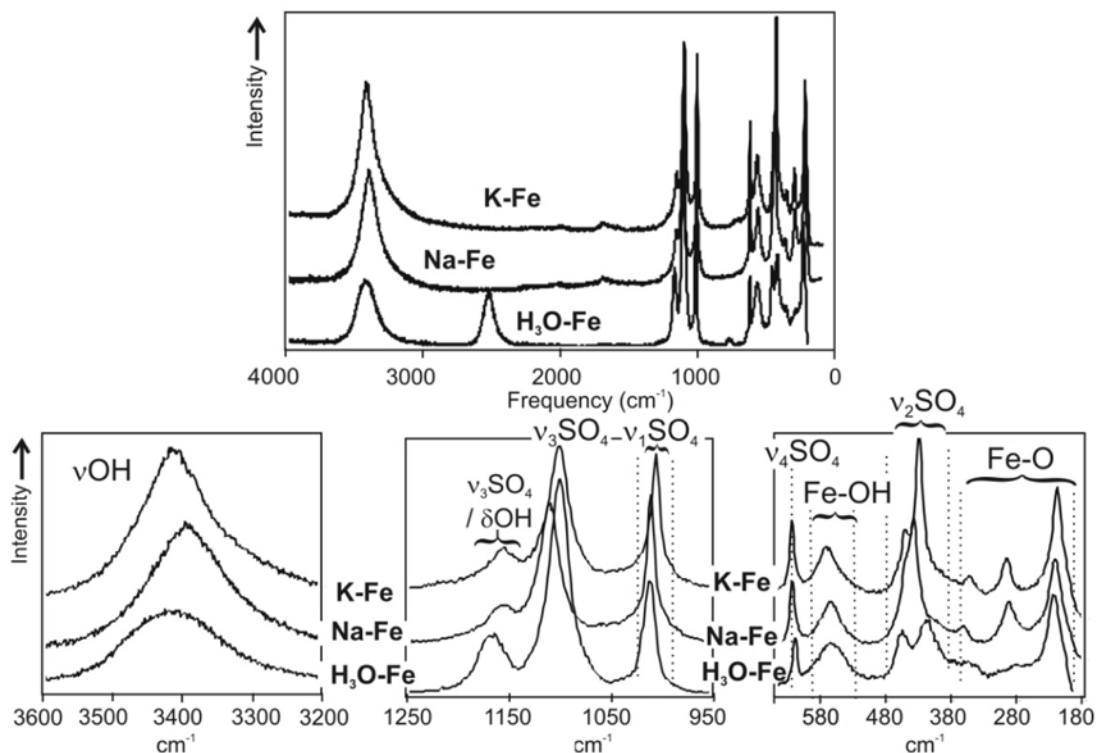


FIG. 4c. Raman spectra of synthetic jarosite-group compounds. See Figure 4a for explanation.

stretches from organic materials that were inadvertently introduced (G. Swayze, pers. commun. 2008).

The Raman-IR differences are more obvious in the intermediate to lower wavenumber ranges. For the K-V alunite-supergroup phase, for example, the Raman spectra show two sharp and clearly defined peaks ($1014.7, 1111.5\text{ cm}^{-1}$) and a much weaker band at 995.1 cm^{-1} (Fig. 6). The IR spectra show three much broader bands, at $1030.2, 1097.0$ and 1188.3 cm^{-1} . The 1014.7 cm^{-1} (Raman) and 1030.2 cm^{-1} (IR) bands, and 1111.5 cm^{-1} (Raman) and 1097.0 cm^{-1} (IR) bands overlap, but their maximum (peak) positions are shifted. In the low-wavenumber region below 700 cm^{-1} , the Raman and IR spectra are completely different (Fig. 6). These differences are likely due to the different responses of Raman and IR to SO_4 and $M-\text{O}$ group symmetries.

Comparison of Raman and IR with XRD

The unit-cell parameters for the alunite- and jarosite-group compounds were compared with the main wavenumbers of the Raman and IR bands. The a parameter correlates well with $v_1\text{SO}_4$, $v_2\text{SO}_4$ and $v_4\text{SO}_4$ Raman wavenumbers (Figs. 7a–c). Only the IR $v_4\text{SO}_4$ wave-

numbers correlate well with the a parameter (Fig. 6d); calculations were not possible for the $v_1\text{SO}_4$, $v_2\text{SO}_4$ or $M-\text{OH}$ wavenumbers because of the lack of identifiable peaks for jarosite-group phases in the IR spectra (Fig. 5, Table 4). The c parameter does not correlate with any of the $v\text{SO}_4$ Raman or IR parameters. Similar relationships between cell dimensions and spectroscopic wavenumbers were recognized by Sasaki *et al.* (1998) and Frost *et al.* (2006b).

Comparison of Raman and IR data with those from other studies

A selection of the Raman wavenumbers for synthetic alunite and natroalunite, and for jarosite, natrojarosite and hydroniumjarosite are compared with previously published Raman wavenumbers (together with the band assignments) in Tables 5 and 6. A similar comparison of IR spectra for these compounds and those from selected other studies is shown in Table 7. The fits for alunite-group and jarosite-group minerals and compounds shown by some authors indicate more peaks than those observed in this study, in particular Frost *et al.* (2006b) in Table 5, (2006a) in Table 6B, and Bishop & Murad

(2005) in Table 7. We do not have a full explanation for this, but suggest that it may be due to differences in preparation and properties (*e.g.*, symmetries) of the synthetic alunite-group and jarosite-group compounds, and especially, spectral peak-fitting procedures.

Despite the differences in absolute numbers of peaks, there is very good agreement in peak wavenumbers between this study and the other investigations, generally within 0.1 to 4 cm⁻¹. Rare exceptions include assignments such as the νOH Raman assignments for synthetic jarosite and natrojarosite (Frost *et al.* 2006a, Table 6) and several of the Raman assignments for the synthetic hydroniumjarosite (Frost *et al.* 2006a, Table 6). Our data thus confirm those in other studies, and highlight the consistency of Raman and IR spectroscopic analysis of alunite and natroalunite, and of jarosite, natrojarosite and hydroniumjarosite.

Use of Raman and IR to distinguish alunite-supergroup phases

We have used Raman and IR spectra of synthetic alunite and natroalunite, and of jarosite, natrojarosite and hydroniumjarosite as the basis for comparison with end-member K-, Na- and H₃O-bearing Cr- and

V-dominant alunite-supergroup compounds, which have not previously been studied by both of these methods. The resultant spectra shown in Figures 4b and 4c, and wavenumbers reported in Tables 3 and 4, show that subtle differences exist among these varieties. No single band allows discrimination between the various compositions, but a comparison between various wavenumbers does allow such differentiation.

The OH stretch around 3400–3500 cm⁻¹ for both Raman and IR is in a different position for all of the alunite-group and jarosite-group compounds and, as discussed above, can be fitted as one or two peaks for the Raman and IR bands. The δOH band only appears in the Raman spectra for alunite-group phases and the Cr analogous compounds, and appears for all of the samples in the IR spectra, where it occurs within a very narrow range of 1631.2 to 1642.5 cm⁻¹. The major differences occur in the νSO_4 and the M–O bands, with respect to the numbers of peaks assigned for each of these bands and shifts in peak position among the compounds. These factors are due to potential errors, non-unique models and differences in the bonding and symmetry in the various synthetic compounds.

Serna *et al.* (1986) did not find any differences in the mid-range wavenumbers of their IR or Raman spectra

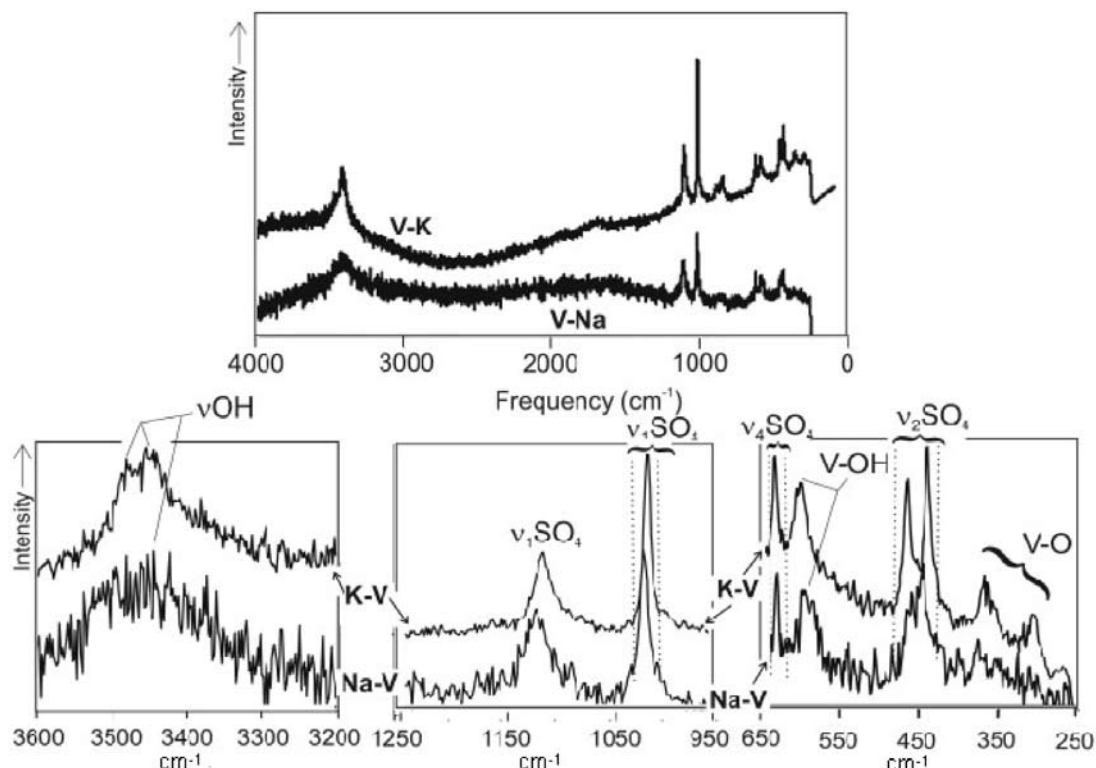


FIG. 4d. Raman spectra of synthetic V-based alunite-supergroup compounds. See Figure 4a for explanation.

TABLE 4. INFRARED (IR) WAVENUMBERS (cm^{-1}) OF ALUNITE-SUPERGROUP COMPOUNDS WITH THE A SITE FILLED WITH K, Na AND H_3O , AND THE B SITE FILLED WITH AI, Cr, Fe AND V

Assignment	K-Al	Na-Al	$\text{H}_3\text{O}-\text{Al}$	K-Cr	Na-Cr	$\text{H}_3\text{O}-\text{Cr}$	K-Fe	Na-Fe	$\text{H}_3\text{O}-\text{Fe}$	K-V	Na-V	$\text{H}_3\text{O}-\text{V}$	
ν_{OH}	3488.3 ^{1,3}	3455.1³	3469.6¹	3434.4	3409.2	3422.7	3384.4^{1,2,3}	3360.4^{1,2,3}	3369.9¹	3412.2	3369.9	3413.2	
ν_{OH}				2925.9			2929.3	3360.0	3388.3			2927.0	
Unassigned							2076.0						
$2\nu_3(\text{SO}_4^{2-})$ or $2\delta\text{OH}$	2233.1 ³	2240.1 ³	2191.3	2122.6	2130.0	2103.1	2024.4	2046.5 ³	2036.2	2041.9	2031.7	2047.0	
$2\nu_3(\text{SO}_4^{2-})$ or $2\delta\text{OH}$							1970.6 ³	1991.0 ³			2007.0		
δOH	1641.8 ³	1638.9 ³	1642.5	1636.4	1634.0	1633.7	1634.8 ³	1637.6 ³	1636.0	1631.2	1633.8	1639.9	
Unassigned					1458.1		1453.0	1455.0				1454.8	
Unassigned						1421.1						1423.7	
Unassigned								1384.9	1394.2			1384.5	
$\nu_3(\text{SO}_4^{2-})$	1230.8 ^{1,3}	1223.1 ³	1228.0 ¹	1211.3	1201.9	1211.6	1184.6 ^{1,2,3}	1186.9 ^{1,2,3}	1186.5 ¹	1188.3	1192.3	1207.7	
Unassigned					1092.1	1101.7	1101.3			1097.0	1106.8	1101.2	
$\nu_3(\text{SO}_4^{2-})$	1083.2^{1,3}	1095.6³	1091.2¹	1051.6	1065.8	1050.8	1087.3^{2,3}	1095.5^{1,2,3}	1090.6¹	1030.2	1041.3	1040.5	
δOH							1022.1 ³						
$\nu_1(\text{SO}_4^{2-})$	1026.2 ¹	1029.1 ¹	1029.4 ¹	1013.9	1019.8	1019.0	1006.0 ²	1010.1 ^{1,2}	1006.7 ¹	1012.5	1016.1		
Unassigned	988.6												
Unassigned	864.7												
Unassigned	842.4												
$\nu_4(\text{SO}_4^{2-})$	670.1^{1,3}	667.4^{1,3}	663.7¹	646.7	648.5	646.5		659.6		701.7			
Unassigned								628.1^{1,2,3}	629.8^{1,2,3}	622.8¹	642.8	641.5	641.9
Unassigned										597.9	606.0		
$\nu_4(\text{SO}_4^{2-})$	623.6 ^{1,3}	628.8 ³	627.0 ¹							592.2	568.2		
γOH	595.3 ^{1,3}	596.2 ^{1,3}	598.4 ¹	555.1	564.4	562.4	574.1 ^{1,2}	565.1 ^{1,2,3}		519.9	514.6	504.8	
M-O	520.3 ³	512.9 ³	516.3 ¹	477.0	475.8	420.3	514.6 ^{1,2,3}	506.9 ³				427.8	
M-O							477.1 ^{1,2,3}	476.0 ³					
$\nu_2(\text{SO}_4^{2-})$	425.8^{1,3}	438.2^{1,3}	427.9¹	404.7	412.3			445.4 ^{1,2}				409.6	

Peak assignments are based on those of Serna *et al.* (1986)¹, Sasaki *et al.* (1998)² and Bishop & Murad (2005)³; assignments for the other alunite-supergroup compounds are inferred.

with different A-site cations (K, Na, H_3O , NH_4) in either jarosite- or alunite-group compounds, but did record differences in the OH-stretching region. They suggested that IR or Raman spectroscopy could distinguish alunite from jarosite, but could not discriminate among various members within each subgroup. By contrast, Sasaki *et al.* (1998) found significant vibrational differences with A-site cation substitution, suggesting that the techniques could be useful for discrimination. In our study, there are differences in the OH-stretching regions, and shifts in the main νSO_4 and M-O peaks of the alunite-group compounds, and Cr-, Fe- and V-dominant alunite-supergroup compounds with substitution of K, Na or H_3O at the A site in the Raman and IR spectra (Figs. 4, 5, Tables 3, 4).

In terms of B-site substitutions, the Cr-, Fe- and V-dominant alunite-supergroup compounds show minor shifts in position and numbers of individual peaks (*e.g.*, arising from δOH , γOH and νSO_4 vibrations) with the same A-site cation. The jarosite-group compounds gave the narrowest (most easily resolved) and most intense Raman spectra (the IR spectra were mostly of similar

intensity and resolution), suggesting that they are the most highly crystalline of the compounds we studied (*cf.* Frost *et al.* 2005a, Hudson-Edwards *et al.* 2008). This characteristic may be because Fe is the heaviest element of the four B-site elements studied, and its resulting stronger bonds may impart differences to the vibrational modes within the compounds with different A-site substitutions. Many previous workers (*e.g.*, Powers *et al.* 1975, Breitinger *et al.* 1998, Drouet *et al.* 2004) have identified significant differences in Raman and IR spectra for alunite- and jarosite-group end-members (regardless of the A-site cation). We too record differences between the alunite- and the jarosite-group compounds. In our IR spectra, most of the alunite-group compound peaks occur at higher values of wavenumber than those for the jarosite-group compounds, which are similar (Table 4). The same differences are observed for the Raman peaks (Table 3), although there is some similarity in the $\nu_1\text{SO}_4$ and lowermost M-O peak positions (Table 3). Breitinger *et al.* (1998) suggested that the difference in OH wavenumber between jarosite- and alunite-group end-members is due to changes in

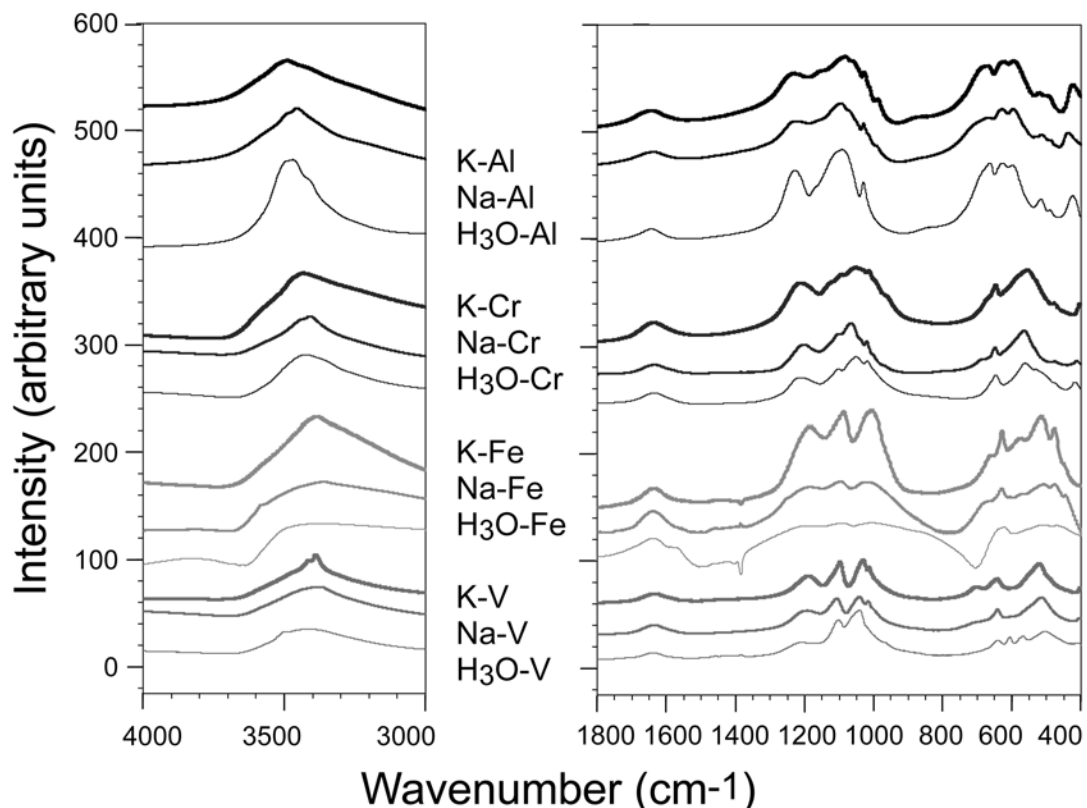


FIG. 5. IR spectra of synthetic alunite- and jarosite-group compounds and V, Cr-bearing analogues.

the bonding of the OH bridging groups to the metal ions, as the lengths of the weak O–H...O hydrogen bonds are the same in both compounds. These results further reveal small but important structural differences between jarosite- and alunite-group compounds, which may arise primarily as a result of the different electronic configuration of Al, compared with that for Cr, Fe and V, which are metals of the first transition series.

CONCLUSIONS

Raman and IR spectroscopies can be used to distinguish synthetic compounds of the alunite supergroup with $A = (\text{Na}^+, \text{K}^+, \text{H}_3\text{O}^+)$ and $B = (\text{Al}, \text{Cr}^{3+}, \text{Fe}^{3+}, \text{V}^{3+})$, and synthesized at temperatures between 25° and 145°C. Differences in the Raman and IR spectra are most significant between the alunite ($B = \text{Al}$) and Cr-, Fe-, and V-based compounds, especially in the νSO_4 and the $M\text{-O}$ band regions. These spectral differences are due to potential errors and variations in the bonding and symmetry in the synthetic compounds, which in turn are related to the different substituting

cations and methods of synthesis. The Raman and IR spectra for each synthetic compound are similar in the high-wavenumber range above 1200 cm^{-1} , but diverge in the intermediate and, especially, low-wavenumber range, below 700 cm^{-1} . These features are likely due to the different responses of Raman and IR to SO_4 and $M\text{-O}$ group symmetries. Our work emphasizes the potential for these types of spectroscopy to be used to characterize other synthetic and natural compounds and minerals of the alunite supergroup.

ACKNOWLEDGEMENTS

This work was funded through a UK Engineering and Physical Sciences Research Council (EPSRC) studentship award (number 309778) to A.M.L. Smith. We thank A.S. Wills for the GSAS refinement, G. Jones and V. Din for assistance with geochemical analyses, and G. Cressey and C. Kirk for help with the XRD analysis. Comprehensive reviews by D. Baron, G. Swayze and an anonymous reviewer greatly helped to improve the manuscript.

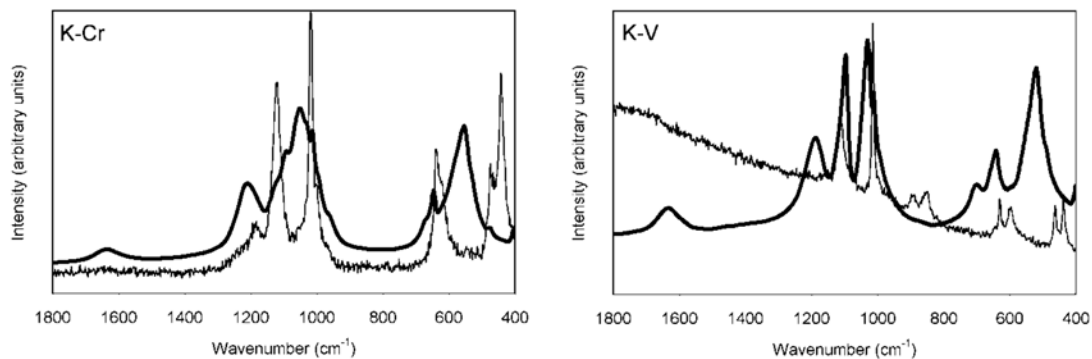


FIG. 6. Comparison of Raman (thin line) and FTIR (thick line) spectra for the K–Cr and K–V alunite-supergroup compounds in the intermediate wavenumber region. Note the slightly shifted overlap of the spectra in the middle range between 1000 and 1200 cm^{-1} , particularly in the K–V compound, and the completely different patterns in the $< 700 \text{ cm}^{-1}$ range.

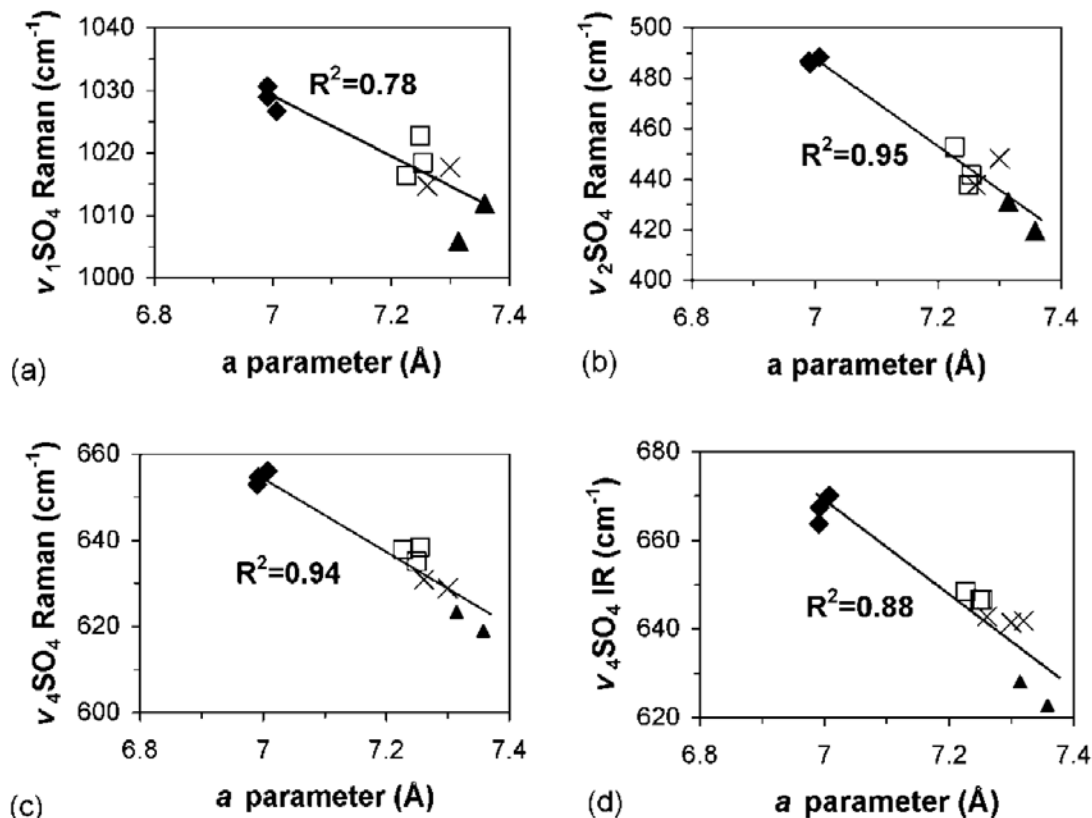


FIG. 7. Correlation of the a unit-cell parameter with selected main Raman and IR wavenumbers. The R^2 values of the linear fits are shown for all plots. Symbols: \blacklozenge alunite-group compounds, \square compounds having Cr at the *B* site, \blacktriangle jarosite-group compounds, \times compounds having V at the *B* site.

TABLE 5. COMPARISON OF MAIN RAMAN WAVENUMBERS (cm^{-1}) FOR SYNTHETIC ALUNITE AND NATROALUNITE WITH DATA FROM FROST *et al.* (2006b)

Assignment	Alunite		Natroalunite	
	This study	F <i>et al.</i> (2006b)	This study	F <i>et al.</i> (2006b)
ν_{OH}	3514.1	3524.5	3487.6	3491.7
Unassigned				3457.0
ν_{OH}	3476.1	3481.7	3446.7	3449.6
Unassigned				3423.8
Unassigned		1228.4		
$\nu_{\text{v}}(\text{SO}_4^{2-})$	1197.4	1194.2		
δOH	1155.1	1158.0	1170.6	1167.5
$\nu_{\text{v}}(\text{SO}_4^{2-})$	1081.9	1082.5	1090.4	1090.5
Unassigned	1052.9	1049.0		
Unassigned				
$\nu_{\text{v}}(\text{SO}_4^{2-})$	1026.7	1026.4	1029.0	1029.9
Unassigned				1027.0
Unassigned	1014.0	1013.6	1016.6	1020.6
γOH	992.5	998.7	997.0	997.5
Unassigned				
Unassigned		989.7		
Unassigned		961.0		
Unassigned		773.3		
$\nu_{\text{v}}(\text{SO}_4^{2-})$	656.1	655.3	654.7	665.3
$\nu_{\text{v}}(\text{SO}_4^{2-})$		644.0		653.6
Unassigned				621.0
$M-\text{O}$ or γOH	563.4	563.1	578.9	575.5
γOH	505.5	504.8	516.4	517.3
Unassigned				513.5
$\nu_{\text{v}}(\text{SO}_4^{2-})$	488.4	488.2	485.9	485.5
Unassigned				403.0
$\nu_{\text{v}}(\text{SO}_4^{2-})$	387.2	388.7	401.7	400.7
Unassigned		373.4		
Unassigned				329.6
$M-\text{O}$ or $\text{OH}-\text{O}$	251.6	248.8		

Assignments for the alunite compounds made for this study are the same as those in Table 3. F *et al.*: Frost *et al.*

REFERENCES

- ADLER, H.H. & KERR, P.F. (1965): Variations in infrared spectra, molecular symmetry, and site symmetry of sulfate minerals. *Am. Mineral.* **50**, 132-147.
- ALPERS, C.N., NORDSTROM, D.K. & BALL, J.W. (1989): Solubility of jarosite solid solutions precipitated from acid mine waters, Iron Mountain, California, U.S.A. *Sci. Géol. Bull.* **42**, 281-298.
- BARON, D. & PALMER, C.D. (2002): Solid-solution aqueous-solution reactions between jarosite ($\text{KFe}_3(\text{SO}_4)_2(\text{OH})_6$) and its chromate analog. *Geochim. Cosmochim. Acta* **66**, 2841-2853.
- BISHOP, J.L. & MURAD, E. (2005): The visible and infrared spectral properties of jarosite and alunite. *Am. Mineral.* **90**, 1100-1107.
- BREITINGER, D.K., MOHR, J., SCHUKOW, H. & SCHWAB, R.G. (1998): Raman spectra of synthetic jarosite-type minerals. In Proc. XVIth Int. Conf. Raman Spectroscopy (A.M. Heyns, ed.). John Wiley and Sons, Supplementary Volume (86-87).
- BREITINGER, D.K., KRIESELSTEIN, R., BOGNER, A., SCHWAB, R.G., PIMPL, T.H., MOHR, J. & SCHUKOW, H. (1997): Vibrational spectra of synthetic minerals of the alunite and crandallite type. *J. Molecular Struct.* **408**, 287-290.

TABLE 6. COMPARISON OF MAIN RAMAN WAVENUMBERS (cm^{-1}) FOR SYNTHETIC JAROSITE-GROUP COMPOUNDS PREPARED FOR THIS STUDY WITH DATA FROM THE LITERATURE

	Synthetic Jrs This study	Synthetic S <i>et al.</i> (1998)	Natural Jrs F <i>et al.</i> (2006a)	Synthetic Njs This study	Synthetic S <i>et al.</i> (1998)	Natural Njs F <i>et al.</i> (2006a)	Synthetic Hjs This study	Natural Hjs F <i>et al.</i> (2006a)
Unassigned								
ν_{OH}	3415.0		3426.1	3395.0		3465.7	3431.0	3452.0
Unassigned						3433.5		
ν_{OH}	3342.0			3277.0		3409.7		3410.9
$\nu_{\text{v}}(\text{SO}_4^{2-})$	1157.6	1153.33	1153.1	1158.6	1154.24	3382.8	3365.0	3383.2
Unassigned						1161.8	1167.7	1154.3
$\nu_{\text{v}}(\text{SO}_4^{2-})$	1101.5	1102.63	1111.0	1110.8	1112.59	1111.5	1100.6	1154.0
Unassigned						1153.5		
$\nu_{\text{v}}(\text{SO}_4^{2-})$	1020.0			1021.0		1010.7	1018.8	1010.1
$\nu_{\text{v}}(\text{SO}_4^{2-})$	1005.9	1006.67	1009.8	1010.8	1012.10	1007.0	1011.8	1007.3
Unassigned								
$\nu_{\text{v}}(\text{SO}_4^{2-})$			998.0					
$\nu_{\text{v}}(\text{SO}_4^{2-})$			632.7	652.4		641.7	632.6	642.6
$\nu_{\text{v}}(\text{SO}_4^{2-})$	623.3	624.61	623.9	622.7	624.61	624.9	619.1	624.3
γOH	569.6	576.63	566.2	565.4	570.29		564.5	573.1
$\nu_{\text{v}}(\text{SO}_4^{2-})$	452.6	453.50	452.8	451.3	450.78	453.9	458.0	453.4
Unassigned			443.7			443.3		
$\nu_{\text{v}}(\text{SO}_4^{2-})$	431.0	434.49	-	438.6	444.44	434.6	419.5	433.6
$M-\text{O}$	354.3	357.53	365.0	364.1	367.49	354.8	358.5	354.2
$M-\text{O}$	299.1	301.40	296.7	294.7	298.68	300.6	281.3	300.6
$M-\text{O}$ or $\text{OH}-\text{O}$	222.2	223.54	225.9	225.6	227.16	227.6	227.1	224.1

Assignments for the jarosite-group compounds made for this study are the same as those in Table 3. Sources of the literature data: S *et al.*: Sasaki *et al.* (1998); F *et al.*: Frost *et al.* (2006a). Naturally occurring samples studied by Frost *et al.* (2006a): jarosite, Jrs: G19611; natrojarosite, Njs: G20148; hydroniumjarosite, Hjs: G23929.

TABLE 7. COMPARISON OF MAIN IR WAVENUMBERS (cm^{-1}) FOR SYNTHETIC ALUNITE, NATROALUNITE, JAROSITE AND NATROJAROSITE FROM THIS STUDY AND FROM THE LITERATURE

Assignment	Alunite		Natroalunite		Jarosite				Natrojarosite			
	This study	B & M (2005)	This study	B & M (2005)	This study	S et al. (1998)	D & N (2003)	B & M (2005)	This study	S et al. (1998)	D & N (2003)	B & M (2005)
ν_{OH}		3515		3487				3410				3400
ν_{OH}	3488.3	3485	3455.1	3456	3384.4	3390	3385	3385	3360.4		3385	3359
ν_{OH}					3365				3360.0	3365		
$2\nu_3(\text{SO}_4^{2-}) / 2\delta\text{OH}$		2293		2313								
Unassigned					2929.3							
$2\nu_3(\text{SO}_4^{2-}) / 2\delta\text{OH}$					2076.0							
$2\nu_3(\text{SO}_4^{2-}) / 2\delta\text{OH}$	2233.1	2227	2240.1	2225	2024.4				2046.5			2195
$2\nu_3(\text{SO}_4^{2-}) / 2\delta\text{OH}$		2183		2143				2178				2167
$2\nu_3(\text{SO}_4^{2-}) / 2\delta\text{OH}$		2124						2105				2120
$2\nu_3(\text{SO}_4^{2-}) / 2\delta\text{OH}$								2078				2086
$2\nu_3(\text{SO}_4^{2-}) / 2\delta\text{OH}$								2024				2046
$2\nu_3(\text{SO}_4^{2-}) / 2\delta\text{OH}$									1991.0			1992
δOH	1641.8	1637	1638.9	1637	1970.6			1967	1637.6		1640	1639
Unassigned					1634.8		1634	1634				
Unassigned					1453.0				1455.0			
$\nu_1(\text{SO}_4^{2-})$	1230.8	1225	1223.1	1222	1184.6	1190	1187	1193	1186.9	1200	1187	1187
$\delta\text{H}_2\text{O}$		1160		1150								
$\nu_1(\text{SO}_4^{2-})$	1083.2	1083	1095.6	1100	1087.3	1088	1088	1085	1095.5	1098	1095	1094
δOH		1070		1061					1022.1			1025
$\nu_1(\text{SO}_4^{2-})$	1026.2	1028	1029.1	1025	1006.0	1028	1007	1005	1010.1	1021	1008	1010
Unassigned	988.6	989*		992*		1010		993*				997*
Unassigned												
Unassigned		864.7										
Unassigned		842.4										
$\nu_4(\text{SO}_4^{2-})$	670.1	668	667.4	666	659.6	660	666	663	675			673
$\nu_1(\text{SO}_4^{2-})$	623.6	622	628.8	628	628.1	630	629	630	629.8	630	629	631
γOH	595.3	594	596.2	597	574.1	580	579		565.1	570		580
M-O	520.3	518	512.9	512	514.6	520	517	508	506.9		509	505
M-O		500	489.9	488	477.1	478	478	474	476.0		476	476
$\nu_2(\text{SO}_4^{2-})$									445.4			445
$\nu_2(\text{SO}_4^{2-})$	425.8	422	438.2	435		448		448				

Sources of the literature data: B & M: Bishop & Murad (2005), S et al.: Sasaki et al. (1998), D & N: Drouet & Navrotzky (2003). * Note that Bishop & Murad (2005) assigned these peaks to $\nu_1(\text{SO}_4^{2-})$, whereas we have adopted the $\nu_1(\text{SO}_4^{2-})$ as shown and left the peaks correlating to * as unassigned. Assignments for the synthetic compounds made for this study are the same as those in Table 4.

BROPHY, G.P. & SHERIDAN, M.F. (1965): Sulfate studies. IV. The jarosite – natrojarosite – hydronium jarosite solid solution series. *Am. Mineral.* **50**, 1595-1607.

DROUET, C. & NAVROTZKY, A. (2003): Synthesis, characterization and thermochemistry of K-Na-H₃O jarosites. *Geochim. Cosmochim. Acta* **67**, 2063-2076.

DROUET, C., PASS, K.L., BARON, D., DRAUCKER, S. & NAVROTZKY, A. (2004): Thermochemistry of jarosite–alunite and natrojarosite–natroalunite solid solutions. *Geochim. Cosmochim. Acta* **68**, 2197-2205.

DUTRIZAC, J.E. & CHEN, T.T. (2003): Synthesis and properties of V³⁺ analogues of jarosite-group minerals. *Can. Mineral.* **41**, 479-488.

DUTRIZAC, J.E. & CHEN, T.T. (2005): Factors affecting the precipitation of chromium(III) in jarosite-type compounds.

Metall. Mater. Trans. B – Process Metall. Mater. Proc. Sci. **36**, 33-42.

DUTRIZAC, J.E. & JAMBOR, J.L. (1984): Formation and characterization of argentojarosite and plumbogjarosite and their relevance to metallurgical processing. In *Applied Mineralogy* (W.C. Park, D.M. Hausen & R.D. Hagni, eds.). Metallurgical Society AIME (American Institute of Mining, Metallurgy and Petroleum Engineers), Littleton, Colorado (507-530).

DUTRIZAC, J.E. & JAMBOR, J.L. (2000): Jarosites and their application in hydrometallurgy. In *Sulfate Minerals – Crystallography, Geochemistry, and Environmental Significance* (C.N. Alpers, J.L. Jambor & D.K. Nordstrom, eds.). *Rev. Mineral. Geochem.* **40**, 405-452.

DUTRIZAC, J.E. & KAIMAN, S. (1976): Synthesis and properties of jarosite-type compounds. *Can. Mineral.* **14**, 151-158.

- ELWOOD MADDEN, M.E., BODNAR, R.J. & RIMSTIDT, J.D. (2004): Jarosite as an indicator of water-limited chemical weathering on Mars. *Nature* **431**, 821-823.
- FROST, R.L., WEIER, M.L., MARTENS, W. & MILLS, S. (2005c): Molecular structure of segnitite: a Raman spectroscopic study. *J. Molec. Struct.* **752**, 178-185.
- FROST, R.L., WILLS, R.-A. & MARTENS, W. (2005b): Raman spectroscopy of beaverite and plumbojarosite. *J. Raman Spectrosc.* **36**, 1106-1112.
- FROST, R.L., WILLS, R.-A., WEIER, M.L. & MARTENS, W. (2005a): Comparison of the Raman spectra of natural and synthetic K- and Na-jarosites at 298 and 77 K. *J. Raman Spectrosc.* **36**, 435-444.
- FROST, R.L., WILLS, R.-A., WEIER, M.L., MARTENS, W. & KLOPROGGE, J.T. (2006b): A Raman spectroscopic study of aluminates. *J. Molec. Struct.* **785**, 123-132.
- FROST, R.L., WILLS, R.-A., WEIER, M.L., MARTENS, W. & MILLS, S. (2006a): A Raman spectroscopic study of selected natural jarosites. *Spectrochim. Acta* **A63**, 1-8.
- GROHOL, D. & NOCERA, D.G. (2002): Hydrothermal oxidation-reduction methods for the preparation of pure and single crystal aluminates: synthesis and characterization of a new series of vanadium jarosites. *J. Am. Chem. Soc.* **124**, 2640-2646.
- GROHOL, D. & NOCERA, D.G. (2007): Magnetic disorder in the frustrated antiferromagnet jarosite arising from the H_3O^+ ... OH^- interaction. *Chem. Mater.* **19**, 3061-3066.
- GROHOL, D., NOCERA, D.G. & PAPOUTSAKIS, D. (2003): Magnetism of pure iron jarosites. *Phys. Rev. B* **67**, 064401.
- HÄRTIG, C., BRAND, P. & BOHMHAMMEL, K. (1984): Fe-Al-Isomorphie und Strukturwasser in Kristallen vom Jarosit-Alunit-Typ. *Z. Anorg. Allg. Chem.* **508**, 159-164.
- HAWTHORNE, F.C., KRIVOVICHEV, S.V. & BURNS, P.C. (2000): The crystal chemistry of sulfate minerals. In *Sulfate Minerals – Crystallography, Geochemistry, and Environmental Significance* (C.N. Alpers, J.L. Jambor & D.K. Nordstrom, eds.). *Rev. Mineral. Geochem.* **40**, 1-112.
- HAYASHI, H. (1994): Mineralogy and chemistry of jarosite and acid sulfate soils. *Nendo Kagaku* **34**, 118-124.
- HENDRICKS, S.B. (1937): The crystal structure of alunite and the jarosites. *Am. Mineral.* **22**, 773-784.
- HUDSON-EDWARDS, K.A., SCHELL, C. & MACKLIN, M.G. (1999): Mineralogy and geochemistry of alluvium contaminated by metal mining in the Rio Tinto area, southwest Spain. *Appl. Geochim.* **14**, 1015-1030.
- HUDSON-EDWARDS, K.A., SMITH, A.M.L., DUBBIN, W.E., BENNETT, A.J., MURPHY, P.J. & WRIGHT, K. (2008): Comparison of the structures of natural and synthetic Pb-Cu-jarosite-type compounds. *Eur. J. Mineral.* **20**, 241-252.
- HUG, S.J. (1997): *In situ* Fourier transform infrared measurements of sulfate adsorption on hematite in aqueous solutions. *J. Colloid Interface Sci.* **188**, 415-422.
- JAMBOR, J.L. (1999): Nomenclature of the alunite supergroup. *Can. Mineral.* **37**, 1323-1341.
- JIANG HUIJIANG & LAWSON, F. (2006): Reaction mechanism for the formation of ammonium jarosite. *Hydrometallurgy* **82**, 195-198.
- KATO, T. & MIURA, Y. (1977): The crystal structures of jarosite and svanbergite. *Mineral. J.* **8**, 419-430.
- KLINGELHÖFER, G., MORRIS, R.V., BERNHARDT, B., SCHRÖDER, C., RODIONOV, D.S., DE SOUZA, P.A., JR., YEN, A., GEL-LERT, R., EVLANOV, E.N., ZUBKOV, B., FOH, J., BONNES, U., KANKELEIT, E., GUTLICH, P., MING, D.W., RENZ, F., WDOWIAK, T., SQUYRES, S.W. & ARVIDSON, R.E. (2004): Jarosite and hematite at Meridiani Planum from Opportunity's Mossbauer spectrometer. *Science* **306**, 1740-1745.
- KUBISZ, J. (1970): Studies on synthetic alkali-hydronium jarosites. I. Synthesis of jarosite and natrojarosite. *Mineral. Polonica* **1**, 47-57.
- LARSON, A.C. & VON DREELE, R.B. (1998): GSAS General Structure Analysis System. Los Alamos National Laboratory, Los Alamos, New Mexico.
- LE BAIL, A., DUROY, H. & FOURQUET, J.L. (1988): Ab initio structure determination of LiSbWO_6 by X-ray powder diffraction. *Mater. Res. Bull.* **23**, 447-452.
- MCMILLAN, P.F. & HOFMEISTER, A.M. (1988): Infrared and Raman spectroscopy. In *Spectroscopic Methods in Mineralogy and Geology* (F.C. Hawthorne, ed.). *Rev. Mineral.* **18**, 99-159.
- MENCHETTI, S. & SABELLI, C. (1976): Crystal chemistry of the alunite series; crystal structure refinement of alunite and synthetic jarosite. *Neues Jahrb. Mineral., Monatsh.*, 406-417.
- OKADA, K., SOGA, H., OSSAKA, J. & OTSUKA, N. (1987): Syntheses of minamite type compounds, $\text{M}_{0.5}\text{Al}_3(\text{SO}_4)_2(\text{OH})_6$ with $\text{M} = \text{Sr}^{2+}$, Pb^{2+} and Ba^{2+} . *Neues Jahrb. Mineral., Monatsh.*, 64-70.
- OMORI, K. & KERR, P.F. (1963): Infrared studies of saline sulfate minerals. *Geol. Soc. Am., Bull.* **74**, 709-734.
- POWERS, D.A., ROSSMAN, G.R., SCHUGAR, H.J. & GRAY, H.B. (1975): Magnetic behaviour and infrared spectra of jarosite, basic iron sulphate and their chromate analogs. *J. Solid State Chem.* **13**, 1-13.
- REWITZER, C. & HOCHLEITNER, R. (1989): Minerals of the old slags from Lavrion, Greece (part 2). *Riv. Mineral. Ital.* **1**, 83-100.
- RIPMEESTER, J.A., RATCLIFFE, C.I., DUTRIZAC, J.E. & JAMBOR, J.L. (1986): Hydronium in the alunite-jarosite group. *Can. Mineral.* **22**, 435-447.



- Ross, S.D. (1974): Sulphates and other oxy-anions of group VI. In *The Infrared Spectra of Minerals* (V.C. Farmer, ed.). The Mineralogical Society, London, UK (423-444).
- RUDOLPH, W.W., MASON, R. & SCHMIDT, P. (2003): Synthetic alunites of the potassium–oxonium solid solution series and some other members of the group: synthesis, thermal and X-ray characterization. *Eur. J. Mineral.* **15**, 913-924.
- SASAKI, K. & KONNO, H. (2000): Morphology of jarosite-group compounds precipitated from biologically and chemically oxidized Fe ions. *Can. Mineral.* **38**, 45-56.
- SASAKI, K., TANAIKE, O. & KONNO, H. (1998): Distinction of jarosite-group compounds by Raman spectroscopy. *Can. Mineral.* **36**, 1225-1235.
- SAVAGE, K.S., BIRD, D.K. & O'DAY, P.A. (2005): Arsenic speciation in synthetic jarosite. *Chem. Geol.* **215**, 473-498.
- SCOTT, K.M. (1987): Solid-solution in, and classification of, goosan-derived members of the alunite–jarosite family, northwest Queensland, Australia. *Am. Mineral.* **72**, 178-187.
- SERNA, C.J., CORTINA, C.P. & RAMOS, J.V.G. (1986): Infrared and Raman study of alunite–jarosite compounds. *Spectrochim. Acta* **42A**, 729-734.
- SHANNON, R.D. (1976): Revised effective ionic radii and systematic studies of interatomic distances in halides and chalcogenides. *Acta Crystallogr.* **A32**, 751-767.
- SMITH, A.M.L., DUBBIN, W.E., WRIGHT, K. & HUDSON-EDWARDS, K.A. (2006a): Dissolution of lead- and lead-arsenic jarosites at pH 2 and 8 and 20°C: insights from batch experiments. *Chem. Geol.* **229**, 344-361.
- SMITH, A.M.L., HUDSON-EDWARDS, K.A., DUBBIN, W.E. & WRIGHT, K. (2006b): Defects and impurities in jarosite: a computer simulation study. *Appl. Geochem.* **21**, 1251-1258.
- SMITH, A.M.L., HUDSON-EDWARDS, K.A., DUBBIN, W.E. & WRIGHT, K. (2006c): Dissolution of jarosite [$\text{KFe}_3(\text{SO}_4)_2(\text{OH})_6$] at pH 2 and 8: insights from batch experiments and computational modelling. *Geochim. Cosmochim. Acta* **70**, 608-621.
- SQUYRES, S.W., KNOLL, A.H., ARVIDSON, R.E., CLARK, B.C., GROTZINGER, J.P., JOLLIFF, B.L., MCLENNAN, S.M., TOSCA, N., BELL, J.F., CALVIN, W.M., FARRAND, W.H., GLOTH, T.D., GOLOMBEK, M.P., HERKENHOFF, K.E., JOHNSON, J.R., KLINGELHÖFER, G., MCSWEEN, H.T. & YEN, A.S. (2006): Two years at Meridiani Planum: results from the Opportunity Rover. *Science* **313**, 1403-1407.
- STOFFREGEN, R.E. & ALPERS, C.N. (1992): Observations on the unit-cell dimensions, H_2O contents, and δD values of natural and synthetic alunite. *Am. Mineral.* **77**, 1092-1098.
- STOFFREGEN, R.E., ALPERS, C.N. & JAMBOR, J.L. (2000): Alunite–jarosite crystallography, thermodynamics, and geochemistry. In *Sulfate Minerals – Crystallography, Geochemistry, and Environmental Significance* (C.N. Alpers, J.L. Jambor & D.K. Nordstrom, eds.). *Rev. Mineral. Geochem.* **40**, 453-479.
- SWAYZE, G.A., DESBOROUGH, G.A., CLARK, R.N., RYE, R.O., STOFFREGEN, R.E., SMITH, K.S. & LOWERS, H.A. (2006): Detection of jarosite and alunite with hyperspectral imaging: prospects for determining their origin on Mars using orbital sensors. Workshop on Martian Sulfates as Recorders of Atmospheric-Fluid – Rock Interactions (Houston), http://www.lpi.usra.edu/meetings/sulfates2006/pdf/download/alpha_m-z.pdf.
- WANG, R., BRADLEY, W.F. & STEINFINK, H. (1965): The crystal structure of alunite. *Acta Crystallogr.* **18**, 249-252.

Received May 30, 2008, revised manuscript accepted June 3, 2009.

